

RESEARCH ARTICLE

Open Access



A high molar activity ^{18}F -labeled TAK-875 derivative for PET imaging of pancreatic β -cells

Mark H. Dornan^{1,2}, Daniil Petrenyov¹, José-Mathieu Simard¹, Antonio Aliaga³, Guoming Xiong³, Julien Ghislain¹, Barry Bedell³, Vincent Poitout^{1,4} and Jean N. DaSilva^{1,2*}

* Correspondence: jean.dasilva@umontreal.ca

¹Centre de Recherche du Centre Hospitalier de l'Université de Montréal, 900 rue St. Denis, Montréal, Québec H2X 0A9, Canada
²Département de radiologie, radio-oncologie et médecine nucléaire, Université de Montréal, 2900 boulevard Edouard-Montpetit, Montréal, Québec H3T 1A4, Canada
Full list of author information is available at the end of the article

Abstract

Background: The free-fatty acid receptor-1 (FFA-1) is expressed by β -cells and is a promising target for molecular imaging of functional β -cell mass. Recently, the ((3- ^{18}F fluoropropyl)sulfonyl)propoxy-derivative of the high-affinity FFA-1 agonist TAK-875 (^{18}F 7) was reported. Here we describe the preparation of this tracer in high molar activity using a purification method permitting separation of ^{18}F 7 from a structurally-related by-product and evaluation of the tracer in rats as a potential FFA-1 PET imaging agent.

Results: The radiotracer was produced by nucleophilic radio-fluorination of the tosylate precursor and deprotection of the methyl ester. Semi-preparative HPLC with a C18 column revealed that ^{18}F 7 co-eluted with a non-radioactive impurity. Mass spectrometry identified the impurity as the alkene-containing elimination by-product. A pentafluorophenyl-functionalized HPLC column was found to separate the two compounds and allowed for purification of ^{18}F 7 in high molar activity. A strong anion-exchange resin was used to reformulate ^{18}F 7 in high concentration. Starting from 96 to 311 GBq of ^{18}F fluoride, 3.8–15.4 GBq of pure ^{18}F 7 (end of synthesis (EOS)) was prepared (RCY $8.3\% \pm 1.1\%$ decay-corrected, $n = 4$) in high molar activity (166–767 GBq/ μmol at EOS). This PET agent was evaluated in rats using dynamic microPET/CT imaging, ex vivo biodistribution, and radio-metabolite studies. MicroPET/CT exhibited high uptake of the tracer in the abdominal area. There was no measurable decrease of the PET signal in the pancreatic area in rats pre-treated with saturating doses (30 mg/kg) of TAK-875. Biodistribution studies corroborated the microPET/CT results. Radiometabolism analyses revealed high compound stability with only the parent molecule detected in the pancreas.

Conclusions: Analysis of the crude reaction mixture and identification of the elimination by-product allowed for the development of a fully automated process to prepare the TAK-875-derived PET agent ^{18}F 7 in high purity and high molar activity. Even though the radiotracer exhibited high in vivo stability, microPET/CT and biodistribution results confirmed recent reports demonstrating that lipophilic analogs of TAK-875 display a high degree of non-specific binding, masking any specific binding to FFA-1 in pancreatic β -cells. Future development of TAK-875-derived PET tracers should focus on reducing non-specific binding in the pancreatic tissue.

Keywords: Pancreatic Beta-cell imaging, Diabetes, Free fatty acid receptor-1, Lipophilic analogs

Background

Type II diabetes mellitus (T2DM) is the predominant form of diabetes. The disease is characterized by insulin resistance and, after an initial compensatory over-production of insulin by β -cells, a loss of β -cell functional mass (Kahn 2003). Current understanding of β -cell dysfunction in T2DM has largely come from post-mortem autopsy data. There have been considerable efforts made towards developing a non-invasive imaging method to monitor β -cell function for both research and clinical studies (Andralojc et al. 2012). Such research would allow better understanding of β -cell mass biology including the pathological mechanisms that lead to depletion during disease progression and could be used in longitudinal studies in the pre-clinical and clinical evaluation of new therapies.

Insulin-secreting β -cells are localized in small (20 to 600 μ M in diameter) clusters of endocrine cells called the islets of Langerhans, which are dispersed throughout the pancreas and account for only 1 to 2% of the total pancreatic mass (Ionescu-Tirgoviste et al., 2015). The size of this anatomical structure and its placement deep within the body restricts potential imaging modalities to those with high sensitivity, spatial resolution, and penetration depth. Given this, nuclear molecular imaging using techniques such as positron emission tomography (PET) or single photon emission computed tomography (SPECT) hold the most promise.

The free fatty acid receptor-1 (FFA-1) is a G-coupled protein receptor that is highly expressed in human and rodent β -cells (Itoh et al. 2003; Briscoe et al. 2002). FFA-1 has attracted significant attention as a potential therapeutic target to promote glucose-stimulated insulin secretion (Mancini and Poitout 2015). The FFA-1 partial agonist TAK-875 was developed as a potent ($K_D = 4.8$ nM and 6.3 nM for human and rat FFA-1, respectively) and selective therapeutic agent that reached phase III clinical trials before development was halted due to liver toxicity (Negoro et al. 2010; Otieno et al. 2017). Structure-activity relationship and TAK-875/FFA-1 co-crystal structure studies suggest that the 3-(methylsulfonyl)propoxy-moiety of TAK-875 could be modified to allow for radionuclide incorporation without significantly impacting target binding (Negoro et al. 2012; Srivastava et al. 2014).

Bertrand and coworkers recently reported the synthesis of TAK-875-derived fluorescent probes for β -cell imaging (Bertrand et al. 2016a). These new probes were used to track specific labeling of cells overexpressing the FFA-1 receptor. Later in 2016, while we were working on the same tracer, Bertrand and coworkers published the radiosynthesis of the ((3-[18 F]fluoropropyl)sulfonyl)propoxy-derivative of TAK-875 ([18 F]7) in 16.7% \pm 5.7% radiochemical yield (RCY) in low molar activity (≥ 0.6 GBq/ μ mol) (Bertrand et al. 2016b). We report here a fully automated process to produce [18 F]7, including optimized HPLC purification and reformulation conditions allowing for removal of the elimination by-product to obtain a high purity, high molar activity, and concentrated formulation of [18 F]7 for in vivo evaluation in rats.

Methods

General

All commercially available materials were used without further purification unless otherwise noted. The synthesis of **1** was completed as previously described (Negoro

et al. 2012). Flash chromatography was carried out with 40–60 μm silica gel. ^1H and ^{13}C NMR spectra were acquired with a 300 MHz spectrometer (Bruker) at ambient temperature. Spectral data is reported in parts per million using residual solvent as a reference. High resolution and accurate mass (HR/AM) measurements were performed in positive and negative ion mode by flow injection analysis into the Thermo Scientific Q-Exactive Plus Orbitrap Mass Spectrometer (San Jose, CA, USA) interfaced with a heated electrospray ion source.

An automated synthesis platform (IBA Synthera[®]) containing two synthesis modules and one semi-preparative radio-HPLC module was used for automated radiotracer production. The production was performed with the Synthera Nucleophilic Integrated Fluidic Processor research and development cassettes (Huayi Isotopes). The cassettes were cleaned with water, ethanol, and dried with nitrogen gas before each usage. Sep-Pak C18 Plus Light cartridges (130 mg, Waters) were pre-conditioned with 10 mL of ethanol followed by 20 mL of deionized water. Sep-Pak QMA Plus Light cartridges (130 mg, Waters) were pre-conditioned by passing through 10 mL of sodium bicarbonate solution (8.4%), followed by 10 mL of deionized water, and drying with helium gas. Semi-preparative HPLC purification was carried out with a Phenomenex Luna PFP (2) column (250 \times 10 mm, 5 μm , flow rate, 8 mL/minute, 50% $\text{CH}_3\text{CN}/\text{H}_2\text{O}$ + 0.1% TFA). A Phenomenex Luna C18 (2) column (250 \times 4.6 mm, 10 μm , flow rate, 2 mL/minute, 35% $\text{CH}_3\text{CN}/\text{H}_2\text{O}$ + 0.1% TFA) was utilized for analytical HPLC with a Waters HPLC equipped with a Raytest Gabi Star radioactivity detector. Residual solvent analyses were conducted using an Agilent 7890B gas chromatograph (headspace sampler).

Chemistry

3-(3-(tert-Butyl-dimethyl-silanyloxy)-propylsulfanyl)-propan-1-ol (2). The product **2** was prepared using a previously published method (Wilke et al. 2014). 3,3'-Thiodipropanol (870 mg, 5.8 mmol) was added to acetonitrile (12 mL) and hexanes (48 mL). Triethylamine (0.97 mL, 6.95 mmol) and tert-butyldimethylsilyl chloride (873 mg, 5.8 mmol) were added and the biphasic mixture was stirred vigorously at room temperature for 8 h. The reaction was quenched with a solution of saturated NH_4Cl and extracted with EtOAc. The combined organic fractions were washed with brine, dried over MgSO_4 , filtered, and concentrated. Compound **2** (903 mg, 3.41 mmol, 59%) was purified by silica column chromatography (10% to 30% EtOAc in hexanes). TLC R_f = 0.44 in 30% EtOAc/hexanes. ^1H NMR (300 MHz, CDCl_3) δ 3.73 (t, J = 6.1 Hz, 2H), 3.67 (t, J = 6.1 Hz, 2H), 2.69–2.52 (m, 4H), 1.97 (s, 1H), 1.89–1.71 (m, 4H), 0.87 (s, 9H), 0.04 (s, 6H). ^{13}C NMR (75 MHz, CDCl_3) δ 61.9, 61.7, 32.7, 32.0, 28.9, 28.6, 26.0, 18.4, –5.2. HRMS (ESI): Exact mass calcd for $\text{C}_{12}\text{H}_{29}\text{O}_2\text{SSi}$ $[\text{M} + \text{H}]^+$: 265.1652. Found: 265.1652.

(S)-methyl-2-(6-((4'-(3-((3-((tert-butyldimethylsilyloxy)-propyl)thio)propoxy)-2',6'-dimethyl-[1,1'-biphenyl]3-yl)methoxy)-2,3-dihydrobenzofuran-3-yl)acetate (3). Compound **1** (950 mg, 2.27 mmol, 1.0 equiv.), **2** (600 mg, 2.27 mmol, 1.0 equiv.), and $P(n\text{-Bu}_3)$ (0.906 mL, 3.63 mmol, 1.6 equiv.) were dissolved in toluene (45 mL). 1,1'-(Azodicarbonyl)dipiperidine (0.916 g, 3.63 mmol, 1.6 equiv.) was added portion wise. The reaction was stirred for 20 h under N_2 atmosphere at room temperature. The reaction mixture was diluted with H_2O and extracted with EtOAc. The desired

compound **3** (1.05 g, 1.585 mmol, 70%) was purified by silica column chromatography (2% to 8% EtOAc in hexanes). TLC R_f = 0.35 in 15% EtOAc/hexanes. ^1H NMR (300 MHz, CDCl_3) δ 7.47–7.34 (m, 2H), 7.17 (s, 1H), 7.08 (d, J = 6.9 Hz, 1H), 7.02 (d, J = 8.0 Hz, 1H), 6.66 (s, 2H), 6.54–6.42 (m, 2H), 5.06 (s, 2H), 4.75 (t, J = 9.0 Hz, 1H), 4.26 (dd, J = 9.1, 6.1 Hz, 1H), 4.08 (t, J = 6.0 Hz, 2H), 3.87–3.75 (m, 1H), 3.75–3.64 (m, 5H), 2.81–2.49 (m, 6H), 2.13–1.95 (m, 8H), 1.88–1.75 (m, 2H), 0.91 (s, 9H), 0.07 (s, 6H). ^{13}C NMR (75 MHz, CDCl_3) δ 172.7, 161.4, 160.3, 158.0, 141.5, 137.7, 137.4, 134.6, 129.5, 129.0, 128.9, 125.8, 124.6, 121.8, 113.5, 107.6, 97.8, 77.9, 70.6, 66.4, 61.9, 52.1, 39.8, 38.1, 33.0, 29.7, 29.0, 28.9, 26.3, 21.4, 18.6, –5.0. Exact mass calcd for $\text{C}_{38}\text{H}_{53}\text{O}_6\text{SSi}$ [$\text{M} + \text{H}$] $^+$: 665.3327. Found: 665.3326.

(S)-methyl-2-(6-((4'-(3-((3-hydroxypropyl)sulfonyl)propoxy)-2',6'-dimethyl-[1,1'-biphenyl]3-yl)methoxy)-2,3-dihydrobenzofuran-3-yl)acetate (4). The compound **3** (275 mg, 0.413 mmol, 1.0 equiv.) was dissolved in CH_3OH (5 mL) and THF (5 mL) and the mixture was cooled to 0 °C. Oxone (254 mg, 0.827 mmol, 2.0 equiv.) dissolved in H_2O (5 mL) was added to the mixture dropwise. The reaction mixture was stirred from 0 °C to room temperature for 18 h. The reaction mixture was concentrated to remove the organic solvent and the aqueous residue was diluted with H_2O . The mixture was extracted with EtOAc, washed with brine, dried over MgSO_4 , filtered, and concentrated. Product **4** (223 mg, 0.383 mmol, 93%) was purified by silica column chromatography (50% to 90% EtOAc in hexanes). TLC R_f = 0.43 in 90% EtOAc/hexanes. ^1H NMR (300 MHz, CDCl_3) δ 7.47–7.33 (m, 2H), 7.16 (s, 1H), 7.07 (d, J = 7.1 Hz, 1H), 7.01 (d, J = 8.0 Hz, 1H), 6.64 (s, 2H), 6.51–6.43 (m, 2H), 5.05 (s, 2H), 4.74 (t, J = 9.0 Hz, 1H), 4.26 (dd, J = 9.2, 6.1 Hz, 1H), 4.12 (t, J = 5.7 Hz, 2H), 3.88–3.74 (m, 3H), 3.71 (s, 3H), 3.32–3.12 (m, 4H), 2.74 (dd, J = 16.4, 5.5 Hz, 1H), 2.55 (dd, J = 16.4, 9.2 Hz, 1H), 2.42–2.28 (m, 2H), 2.21–2.07 (m, 2H), 1.99 (s, 6H), 1.72 (s, 1H). ^{13}C NMR (75 MHz, CDCl_3) δ 172.7, 161.4, 160.2, 157.4, 141.2, 137.9, 137.5, 135.1, 129.4, 129.0, 128.9, 125.9, 124.6, 121.8, 113.5, 107.6, 97.8, 77.9, 70.6, 65.7, 60.9, 52.1, 50.4, 50.3, 39.8, 38.1, 25.3, 22.7, 21.4. HRMS (ESI): Exact mass calcd for $\text{C}_{32}\text{H}_{39}\text{O}_8\text{S}$ [$\text{M} + \text{H}$] $^+$: 583.2360. Found: 583.2366.

(S)-methyl-2-(6-((2',6'-dimethyl-4'-(3-((3-(tosyloxy)propyl)sulfonyl)propoxy)-[1,1'-biphenyl] 3-yl)methoxy)-2,3-dihydrobenzofuran-3-yl)acetate (5). Product **5** was prepared as described previously (Bertrand et al. 2016b). *p*-Toluenesulfonyl chloride (196 mg, 1.03 mmol, 1.5 equiv.) dissolved in 1.9 mL of CH_2Cl_2 was added dropwise to a solution of **4** (400 mg, 0.686 mmol, 1.0 equiv.) dissolved in toluene (4.7 mL) and CH_2Cl_2 (4.7 mL), in the presence of triethylamine (0.143 mL, 1.03 mmol, 1.5 equiv.) and *N,N,N',N'*-tetramethyl-1,6-hexanediamine (15 μL , 0.0686 mmol, 0.1 equiv.). The reaction was stirred for 18 h at room temperature. The mixture was quenched with H_2O , extracted with EtOAc, washed with brine, dried over MgSO_4 , filtered and concentrated. The product **5** (463 mg, 0.628 mmol, 92%) was purified by silica column chromatography (30% to 50% EtOAc in hexanes). TLC R_f = 0.40 in 50% EtOAc/hexanes. ^1H NMR (300 MHz, CDCl_3) δ 7.79 (d, J = 8.3 Hz, 2H), 7.46–7.32 (m, 4H), 7.16 (s, 1H), 7.07 (dt, J = 7.1, 1.6 Hz, 1H), 7.02 (d, J = 8.0 Hz, 1H), 6.64 (s, 2H), 6.52–6.43 (m, 2H), 5.06 (s, 2H), 4.75 (t, J = 9.0 Hz, 1H), 4.26 (dd, J = 9.2, 6.1 Hz, 1H), 4.19 (t, J = 5.9 Hz, 2H), 4.11 (t, J = 5.7 Hz, 2H), 3.87–3.74 (m, 1H), 3.71 (s, 3H), 3.28–3.16 (m, 2H), 3.16–3.05 (m, 2H), 2.75 (dd, J = 16.4, 5.5 Hz, 1H), 2.55 (dd, J = 16.4, 9.2 Hz, 1H), 2.46 (s, 3H), 2.38–2.19 (m, 4H), 1.99 (s, 6H). ^{13}C NMR (75 MHz, CDCl_3) δ 172.6, 161.4, 160.2, 157.4, 145.6, 141.2, 137.9, 137.5, 135.2, 132.9, 130.4, 129.4, 129.0, 128.9, 128.3, 125.9, 124.6,

121.8, 113.5, 107.6, 97.8, 77.9, 70.6, 68.3, 65.6, 52.1, 50.7, 49.4, 39.8, 38.1, 22.6, 22.2, 22.0, 21.4. Exact mass calcd for $C_{39}H_{45}O_{10}S_2$ $[M + H]^+$: 737.2449. Found: 737.2442.

(S)-methyl-2-(6-((2',6'-dimethyl-4'-(3-(3-fluoropropyl)sulfonyl)propoxy)-[1,1'-biphenyl] 3-yl)methoxy)-2,3-dihydrobenzofuran-3-yl)acetate (6). Product **6** was prepared as described previously (Bertrand et al. 2016b). 50% Deoxo-fluor (bis(2-methoxyethyl)aminosulfur trifluoride) in THF (37 mg, 0.166 mmol, 1.65 equiv.) was added to **4** (59 mg, 0.101 mmol, 1.0 equiv.) in CH_2Cl_2 at 0 °C. The reaction was allowed to react from 0 °C to room temperature for 18 h. The reaction mixture was diluted with H_2O , extracted with EtOAc, dried over Na_2SO_4 , filtered and concentrated. The desired product **6** (31 mg, 0.053 mmol, 53%) was purified by silica column chromatography (20% to 50% EtOAc in hexanes). TLC R_f = 0.51 in 50% EtOAc/hexanes. 1H NMR (300 MHz, $CDCl_3$) δ 7.46–7.34 (m, 2H), 7.16 (s, 1H), 7.07 (d, J = 7.0 Hz, 1H), 7.02 (d, J = 8.0 Hz, 1H), 6.64 (s, 2H), 6.52–6.44 (m, 2H), 5.05 (s, 2H), 4.75 (t, J = 9.0 Hz, 1H), 4.68 (t, J = 5.6 Hz, 1H), 4.53 (t, J = 5.6 Hz, 1H), 4.26 (dd, J = 9.2, 6.1 Hz, 1H), 4.13 (t, J = 5.7 Hz, 2H), 3.86–3.74 (m, 1H), 3.72 (s, 3H), 3.29–3.14 (m, 4H), 2.75 (dd, J = 16.4, 5.5 Hz, 1H), 2.55 (dd, J = 16.4, 9.2 Hz, 1H), 2.42–2.19 (m, 4H), 1.99 (s, 6H). ^{13}C NMR (75 MHz, $CDCl_3$) δ 172.67, 161.45, 160.25, 157.40, 141.25, 137.98, 137.49, 135.18, 129.45, 128.99, 128.89, 125.94, 124.61, 121.83, 113.52, 107.63, 97.79, 82.01 (d, $J_{C,F}$ = 168 Hz), 77.90, 70.61, 65.70, 52.13, 50.59, 49.55 (d, $J_{C,F}$ = 4 Hz), 39.81, 38.09, 23.57 (d, $J_{C,F}$ = 21 Hz), 22.67, 21.45. HRMS (ESI): Exact mass calcd for $C_{32}H_{39}O_{8}S$ $[M + Na]^+$: 607.2136. Found: 607.2136.

(S)-2-(6-((4'-(3-(3-fluoropropyl)sulfonyl)propoxy)-2',6'-dimethyl-[1,1'-biphenyl]3-yl)methoxy)-2,3-dihydrobenzofuran-3-yl)acetic acid (7). Product **7** was prepared as described previously (Bertrand et al. 2016b). $NaOH_{(aq)}$ (1.0 M, 0.17 mL) was added to a solution of **6** (20 mg, 0.034 mmol, 1.0 equiv.) in CH_3OH (0.3 mL) and THF (0.6 mL), and the mixture was heated to 50 °C for 1 h. The reaction mixture was concentrated and **7** (17.3 mg, 0.030 mmol, 88%) was purified by silica column chromatography (80% EtOAc in hexanes + 0.5% CH_3CO_2H). TLC R_f = 0.40 in 80% EtOAc/hexanes + 0.5% CH_3CO_2H . 1H NMR (300 MHz, $CDCl_3$) δ 7.47–7.33 (m, 2H), 7.16 (s, J = 10.1 Hz, 1H), 7.06 (t, J = 7.4 Hz, 2H), 6.64 (s, 2H), 6.53–6.43 (m, 2H), 5.05 (s, 2H), 4.75 (t, J = 9.0 Hz, 1H), 4.68 (t, J = 5.6 Hz, 1H), 4.53 (t, J = 5.6 Hz, 1H), 4.28 (dd, J = 9.2, 6.1 Hz, 1H), 4.12 (t, J = 5.7 Hz, 2H), 3.87–3.72 (m, 1H), 3.30–3.13 (m, 4H), 2.80 (dd, J = 16.7, 5.2 Hz, 1H), 2.60 (dd, J = 16.7, 9.3 Hz, 1H), 2.41–2.28 (m, 3H), 2.28–2.19 (m, 1H), 1.99 (s, 6H). ^{13}C NMR (75 MHz, $CDCl_3$) δ 161.43, 160.31, 157.40, 141.26, 137.98, 137.45, 135.17, 129.48, 129.00, 128.89, 125.94, 124.63, 121.58, 113.53, 107.72, 97.84, 82.0 (d, $J_{C,F}$ = 168 Hz), 70.62, 65.70, 50.58, 49.55 (d, $J_{C,F}$ = 4 Hz), 37.91, 23.56 (d, $J_{C,F}$ = 21 Hz), 22.65, 21.45. Exact mass calcd for $C_{31}H_{35}FNaO_7S$ $[M + Na]^+$: 593.1980. Found: 593.1984.

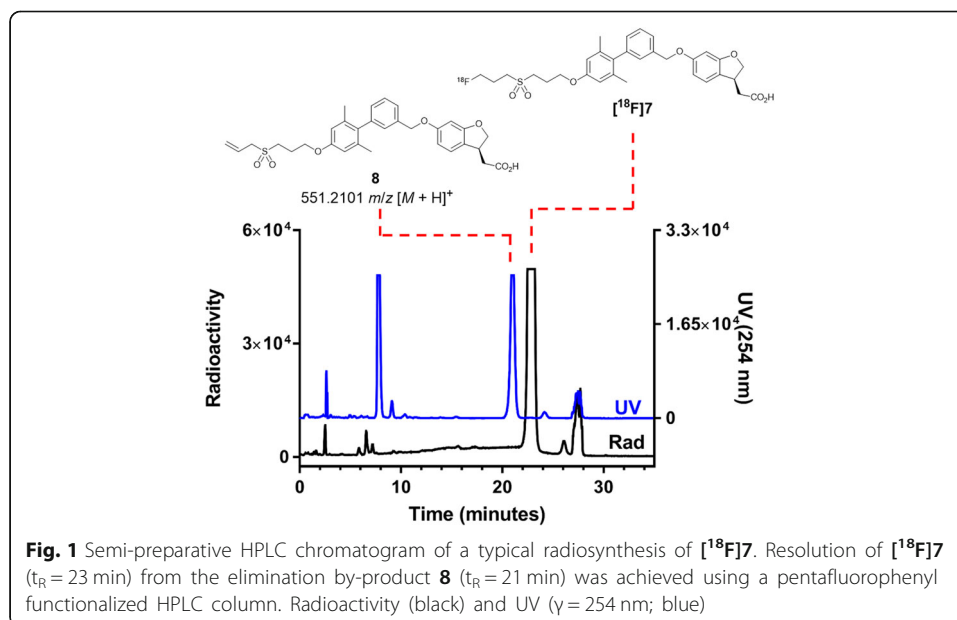
Production of [^{18}F]7

Using an IBA Cyclone[®] 18/9 cyclotron, [^{18}F]fluoride was produced by the $^{18}O(p,n)^{18}F$ nuclear reaction and was transferred to the IBA Synthra[®] radiochemistry platform which was configured with two synthesis units and an HPLC module. The [^{18}F]fluoride was trapped on a pre-conditioned Waters Sep-Pak[®] QMA Plus Light anion-exchange cartridge. [^{18}F]Fluoride was eluted from the cartridge into the reactor with 0.6 mL of a 1:1 mixture of acetonitrile/water containing 2.2.2-cryptand (22.6 mg)

and potassium carbonate (4.2 mg). Acetonitrile was added, and the mixture was azeotropically dried under vacuum and heat. A solution of the tosylate precursor **5** (5 mg) in 1 mL of acetonitrile was added and the reactor was heated to 100 °C for 2.5 min. Following removal of the solvent (vacuum), the reactor was cooled and 1 mL of a 1:1 mixture of aqueous NaOH (2.5 M)/CH₃OH was added. After 3 min, the reaction was quenched with 10 mL of H₂O + 0.1% TFA and transferred through a pre-conditioned Waters Sep-Pak® C18 cartridge. Acetonitrile (1.2 mL) eluted the radiotracer from the C18 cartridge into a V-vial containing H₂O + 0.1% TFA (1.8 mL) and injected onto semi-preparative HPLC equipped with a Phenomenex Luna PFP (2) column, which enabled separation of the radiotracer from the elimination by-product **8** (Fig. 1). The fraction containing [¹⁸F]**7** was collected into a vessel containing aqueous NaOH (1.0 M, 30 mL) and transferred over a Waters Oasis® MAX anion-exchange resin cartridge using vacuum and N₂ push in the second Synthra synthesis unit. Following deionized water wash (10 mL), [¹⁸F]**7** was eluted with 1 mL EtOH + 0.5% HCl, then filtered (0.22 μm) into a sterile multidose vial containing 9 mL of isotonic bicarbonate-buffered saline. Analytical HPLC was performed to determine the chemical and radiochemical purity. Identity of [¹⁸F]**7** was determined by HPLC co-elution with the non-radioactive standard **7**. The molar activity was measured by comparing the UV (254 nm) peak of [¹⁸F]**7** with an injection of the non-radioactive standard **7** with a comparable UV response.

Identification of the impurity **8**

The radiosynthesis and HPLC purification of [¹⁸F]**7** was conducted as described above using a semi-preparative Phenomenex Luna C18 column. The HPLC peak containing a co-elution of [¹⁸F]**7** and a non-radioactive impurity was collected. The decayed fraction was diluted in methanol and analyzed by mass spectrometry. HRMS (ESI): Exact mass calcd for C₃₁H₃₅O₇S [M + H]⁺: 551.2098. Found: 551.2101.



Animals

Male Sprague-Dawley rats (150–175 g, Charles River Laboratories, Montreal, Canada) were housed on a 12 h:12 h light/dark cycle and fed standard rat chow and water ad libitum. This study was carried out in accordance with Canadian Council on Animal Care guidelines. The protocol (protocol number IM16029JDSr) was approved by the institutional Animal Care Committees of the Centre de Recherche du Centre Hospitalier de l'Université de Montreal and the McGill University Health Centre.

Small animal PET imaging

General

Small animal PET/CT scans were performed with [^{18}F]7 (7.4–14.8 MBq, 0.12–0.66 μg non-radioactive mass) in control animals ($n = 3$) on a Mediso nanoScan PET/CT (Mediso Medical Imaging Systems, Budapest, Hungary). To assess binding specificity to FFA-1 in the pancreas, additional rats ($n = 3$) were injected with TAK-875 (30 mg/kg, from a 20 mg/mL solution of TAK-875 in 10,5,1 saline 0.9%/H₂O/sodium bicarbonate 8.4% + 10% DMSO) intravenously 5 min before administration of [^{18}F]7 (12.8–13.5 MBq, 0.27–0.58 μg non-radioactive mass).

Image acquisition

Each PET/CT session consisted of a 60 min PET emission scan, followed by a 10 min CT transmission scan. PET/CT scans were conducted under anesthesia (isoflurane 2%, oxygen 0.6 L/min) delivered by a nose cone. Temperature and heart rate were monitored throughout the procedure using the Mediso system. After the animal was placed in the scanner, with the heart positioned at the center of the field of view, emission scans were initiated immediately after a bolus injection in the tail vein. List mode data was histogrammed into 29 sequential time frames of increasing duration (6 \times 10 s, 4 \times 30 s, 4 \times 60 s, 4 \times 120 s, 5 \times 180 s, 6 \times 300 s frames) over 60 min. Images were reconstructed using expectation maximization (EM), ordered subset expectation maximization (OSEM), normalized, and corrected for scatter, dead time, and decay.

Image analysis

Images were analyzed with Amide software (version 1.0.5 for Linux). Regions of interest (ROI) were defined on reconstructed images in the pancreas, kidney, liver and muscle to obtain time-activity curves. A 3-D sphere with a radius of 2.5 mm was drawn within the left ventricle using an average image of very early frames (10–60 s) to sample the blood input function. The sphere was centred at the point where the maximum activity was found inside this region. The ROIs for pancreas, kidney, liver and muscle were drawn using an average image of early frames (1–20 min post injection where highest tissue to background contrast can be obtained). For kidney and liver, the ROIs are 3-D spheres located roughly in the middle of the tissue with a radius of 5 mm (kidney) and 6 mm (liver), respectively. For pancreas, the ROI was ellipsoid shaped and was created based on the anatomy of rats as both CT and PET images could not help with distinguishing this tissue from other organs.. The radii of the

ROI were 1.5 mm (sagittal), 3 mm (transverse), and 3 mm (coronal), respectively. For muscle, the ROI was a 3-D sphere located on the muscle near left shoulder of the animals with a radius of 3 mm.

Statistical analysis

Results are presented as mean \pm standard deviation. A two-tailed t-test was used to compare between two groups. *P* values < 0.05 were considered significant.

Biodistribution studies

Biodistribution studies were performed to evaluate tissue uptake and to measure specific and non-specific binding of the radiotracer to FFA-1. Briefly, rats were anesthetized (2–2.5% isoflurane) and injected via a lateral tail vein with 7.8–12.2 MBq tracer activity. Baseline group animals ($n = 4$) received tracer alone, whereas the blocking group animals ($n = 4$) received an intravenous dose of the FFA-1 agonist TAK-875 (30 mg/kg) 5 min prior to tracer administration. Rats were sacrificed by decapitation at 20 min post-injection. Trunk blood was collected in heparinized tubes. The following tissues were dissected and collected into pre-weighed tubes: pancreas, kidney, spleen, fat, bone, muscle, blood, plasma. Using a gamma counter (PerkinElmer Wizard2), all tubes were counted along with a 1:100 dilution of the injected tracer solution as a standard. The percent of the injected dose per gram of tissue (%ID/g) was calculated from the decay-corrected counts and expressed as a ratio to blood.

Radiolabeled metabolite analysis

General

Radiolabeled metabolite analysis studies were performed to evaluate the metabolic stability of [^{18}F] in plasma and the pancreas. Rats were anesthetized (2–2.5% isoflurane) and injected via the lateral tail vein with 35.2–73.3 MBq of [^{18}F]. At 60-min post-injection, the animals were sacrificed by decapitation. Trunk blood was collected into heparinized tubes and the pancreas was dissected.

Sample preparation

Blood was centrifuged (4000 \times g, 5 min, 4 $^{\circ}\text{C}$) to obtain plasma. Urea (1 g) was dissolved in the plasma (1 mL) and the sample was filtered (0.22 μm) and injected onto the column-switching HPLC. Pancreas samples were suspended in 80:20 EtOH/H₂O, homogenized using a polytron and centrifuged (14.8 rpm, 20 min, 4 $^{\circ}\text{C}$). The supernatant was collected and dried by rotary evaporation. The residue was reconstituted in 1 mL of 1% CH₃CN/H₂O containing 0.4 g of urea to reduce protein binding, filtered (0.22 μm), and injected onto the column-switching HPLC. Most of the radioactivity from the pancreas (and plasma) was present in the injected sample.

Column-switching HPLC

A modification of the column-switching HPLC procedure was used (Kenk et al. 2008) to analyse the radioactive metabolites from plasma and pancreas samples. Eluted solvents were analyzed via two detectors in series: a UV absorbance detector (Waters 2489) and a radiation detector (Raytest Gabi Star), which were connected to a

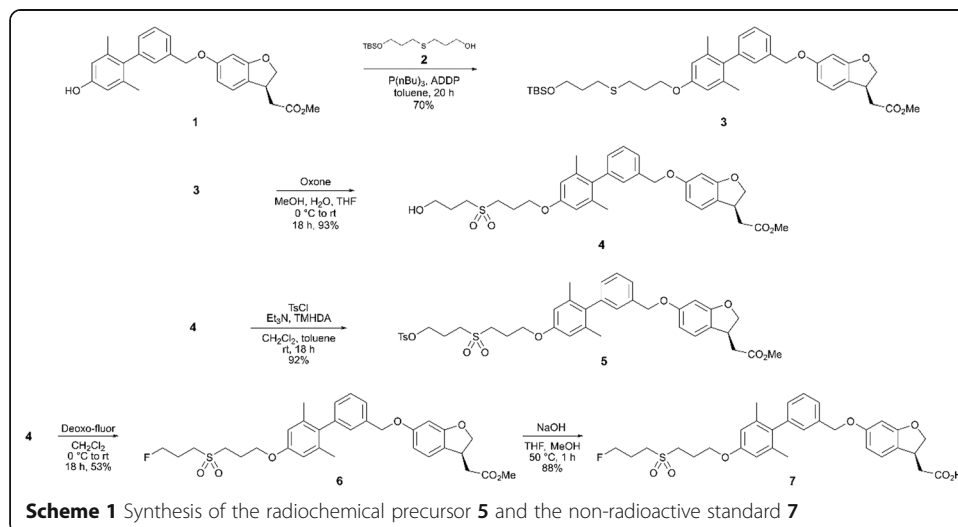
chromatography data integration system (PeakSimple, using PeakSimple data analysis software, version 4.44). Using mobile solvent A (1% CH₃CN/H₂O + 0.1% TFA, 1 or 2 mL/minute), samples were loaded onto an in-line refillable capture column (hand-packed with 20 mg of Oasis HLB polymeric reverse phase sorbent) fitted with 2.5 μm frits. The elution of biological macromolecules was monitored by UV absorbance (254 nm) and radioactivity. When the UV signal returned to baseline, the solvent flow was switched to elute the capture column loaded sample onto the analytical column (Phenomenex Luna C18, 250 × 4.6 mm, 10 μm) using mobile Solvent B (65% CH₃CN/H₂O + 0.1% TFA, 2 mL/minute flow rate). Retention times were calculated from the time of switch. Radioactivity data are expressed as the percentage of the total radioactivity signal. For standards, samples of blood and pancreas from control rats were spiked with [¹⁸F]7 and processed as described above for each formulation tested. Use of such controls allowed for measurement of the proportion of radiotracer retained and not-retained by the capture column during loading. If radioactivity was eluted during loading of the capture column, this activity will be identified as authentic [¹⁸F]7 and not as a hydrophilic labeled metabolite.

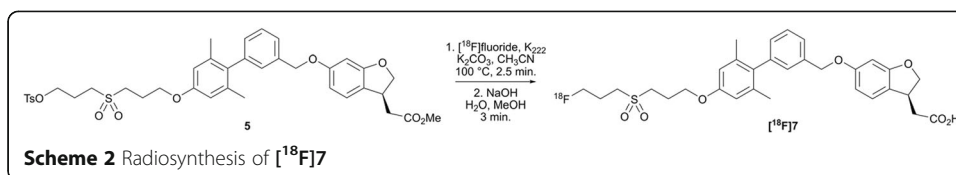
Results

Chemistry and radiochemistry

The monoprotected diol **2** was synthesized following a literature procedure (Wilke et al. 2014). A Mitsunobu coupling reaction was used to synthesize **3** in 70% yield. Treatment of **3** with Oxone oxidized the thioether to a sulfone and deprotected the terminal alcohol protecting group to afford **4** in 93% yield (Scheme 1). Tosylation of **4** provided the radiochemical precursor **5** in 92% yield. To produce the non-radioactive standard **7**, the compound **4** was treated with Deoxo-Fluor (bis(2-methoxyethyl)aminosulfur trifluoride) followed by base-mediated ester hydrolysis, as described before (Bertrand et al. 2016b).

The radiosynthesis of [¹⁸F]7 was performed with an automated one-pot, two-step procedure. [¹⁸F]fluoride nucleophilic displacement of the tosylate leaving group was followed by base-mediated hydrolysis of the methyl ester (Scheme 2). The quenched





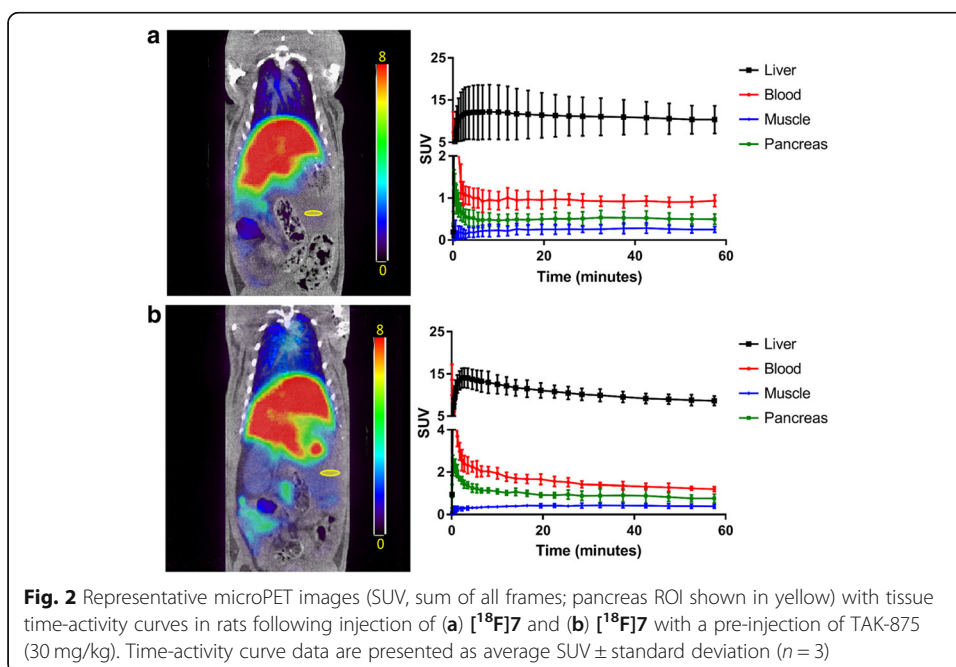
reaction mixture was purified by C18 SPE cartridge followed by semi-preparative HPLC (Fig. 1). The peak corresponding to [^{18}F]7 was collected into a vessel containing aqueous NaOH, loaded onto a weak anionic exchange resin, then eluted with acidified ethanol into isotonic bicarbonate-buffered saline. This procedure allowed for rapid reformulation in high concentration. Starting from 96 to 311 GBq of [^{18}F]fluoride, 3.8–15.4 GBq of [^{18}F]7 (at EOS) was prepared (decay-corrected RCY 8.3% \pm 1.1%, $n = 4$) in 75–89 min. The molar activity ranged from 166 to 767 GBq/ μmol at EOS.

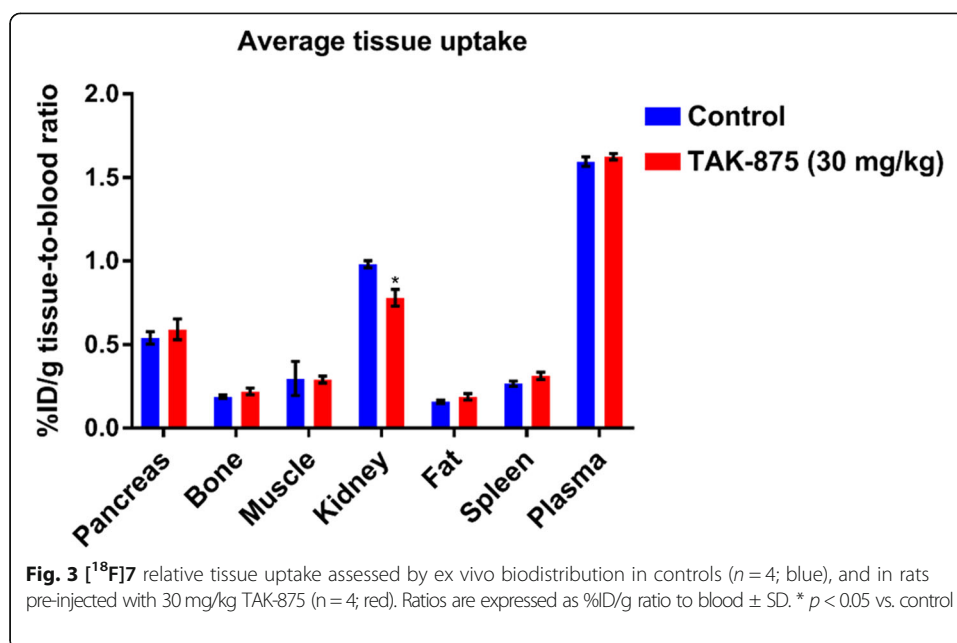
MicroPET imaging

Preliminary microPET/CT scans performed with [^{18}F]7 exhibited the highest radiotracer concentration in the liver (Fig. 2). At 10 min post-injection, control group tissue-to-blood ratios for the liver, kidney and pancreas were 12.34 ± 3.34 , 0.62 ± 0.07 , and 0.49 ± 0.05 , respectively ($n = 3$). In the TAK-875 pre-treated group, tissue-to-blood ratios in the liver, kidney and pancreas were 6.50 ± 0.96 , 0.66 ± 0.04 , and 0.57 ± 0.09 , respectively ($n = 3$).

Ex vivo biodistribution

The average % ID/g tissue-to-blood ratios for the control and blocked groups are presented in Fig. 3. In the control group, the highest average activity concentrations were found in the plasma, kidney, and pancreas (average tissue-to-blood ratios 1.60 ± 0.03 ,





0.98 ± 0.02 , and 0.54 ± 0.04 , respectively; $n = 3$). Lower activity concentrations were detected in the muscle, spleen, bone, and fat tissue samples (average tissue-to-blood ratios 0.30 ± 0.1 , 0.27 ± 0.02 , 0.19 ± 0.01 , and 0.16 ± 0.01 , respectively; $n = 3$). Blocking the FFA-1 receptor did not result in any significant difference in the tissue average activity concentrations except for the kidney, which was reduced by 20% ($P < 0.05$).

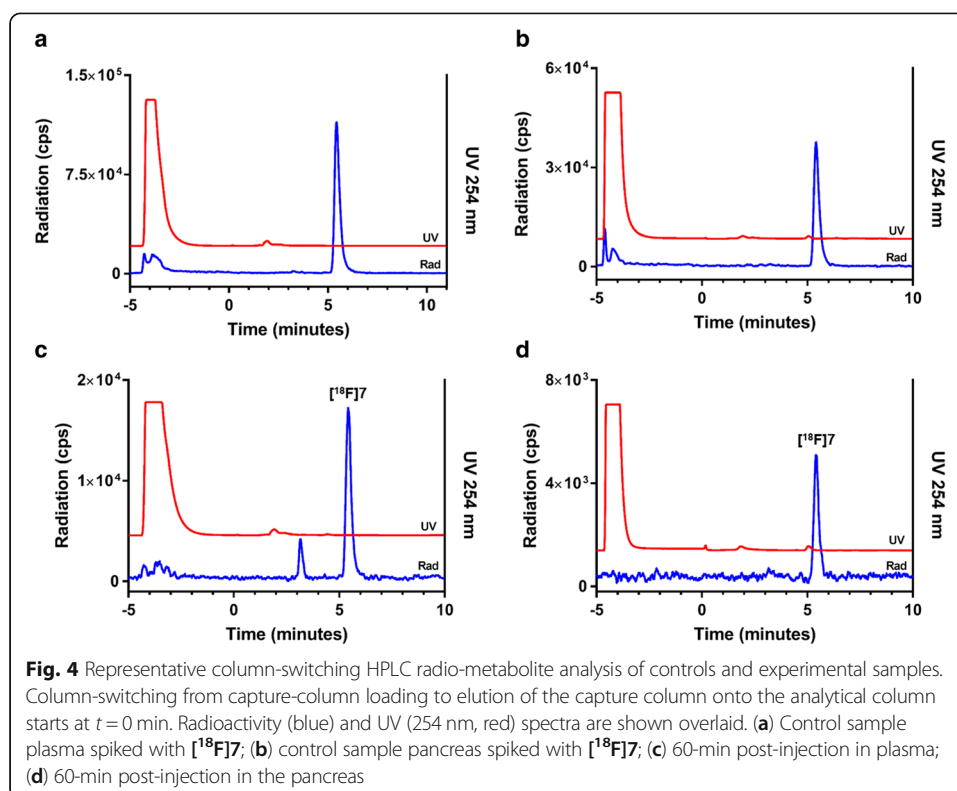
Radiolabeled metabolites analysis

Column-switching HPLC analysis of the control plasma and pancreas samples spiked with authentic [^{18}F]7 revealed only one peak, corresponding to unchanged tracer ($R_t = 5.5$ min) (Fig. 4a-b). This demonstrated that the tissue processing method did not degrade or affect the radiotracer. No other peaks were detected in the control samples.

Sixty minutes following intravenous administration of [^{18}F]7 in rats ($n = 4$), one labeled hydrophilic metabolite was observed in rat plasma after the switch ($R_t = 3.1$ min) on analytical HPLC, while $88\% \pm 4\%$ of the total radioactivity was attributed to unchanged radiotracer (Fig. 4c). In the pancreas homogenate, only the unchanged radiotracer was detected ($n = 4$) (Fig. 4d).

Discussion

A novel automated method was developed to produce the ((3- ^{18}F)fluoropropyl)sulfonyl-propoxy-derivative of TAK-875 ([^{18}F]7) in high molar activity and purity, allowing for in vivo evaluation in rats as a potential FFA-1 probe for β -cell PET imaging. The tosylate precursor **5** and the non-radioactive standard **7** were synthesized starting from the aromatic alcohol **1**. The thioether intermediate **3** was produced by coupling the mono-protected diol **2** with the aromatic alcohol **1** using Mitsunobu-coupling conditions. Removal of the silyl protecting group and oxidation of the thioether was achieved in a single step by treatment with Oxone to give **4**. The radiochemical precursor **5** was generated by tosylation of **4** as described previously (Bertrand et al. 2016b). The non-radioactive



standard was synthesized by fluorination of **4** using Deoxo-Fluor, followed by base-mediated ester hydrolysis (Bertrand et al. 2016b).

The radiosynthesis of $[^{18}\text{F}]7$ was completed with a nucleophilic radio-fluorination reaction followed by base-mediated ester hydrolysis in a one-pot, two-step process. Semi-preparative HPLC purification of $[^{18}\text{F}]7$ was initially explored using a C18 column. Co-elution of the radiotracer with a non-radioactive by-product was observed. Despite efforts, chromatographic resolution of the tracer from this by-product was not achieved by adjusting the mobile phase composition. High resolution mass spectrometry indicated that the identity of the impurity was the alkene-containing elimination by-product **8** (Fig. 1). Resolution of $[^{18}\text{F}]7$ from **8** was achieved employing a pentafluorophenyl-functionalized reverse phase column which enabled preparation of $[^{18}\text{F}]7$ in high purity. Inspection of previously described structure-activity relationships and the TAK-875/FFA-1 co-crystal structure predicted that **8** would potentially compete with $[^{18}\text{F}]7$ for binding to FFA-1 (Negoro et al. 2012; Srivastava et al. 2014). Thus, removal of **8** will increase the apparent molar activity of the final product and improve the potential for quantitative PET imaging of pancreatic FFA-1 and β -cell mass.

Reformulation of $[^{18}\text{F}]7$ was performed using an anion exchange resin. The purified $[^{18}\text{F}]7$ HPLC peak was collected into a vessel containing aqueous base to ensure ionization of the carboxylic acid functional group. From this solution, the carboxylate form of $[^{18}\text{F}]7$ was efficiently captured by the resin. The residual HPLC solvent was removed by washing with water. The radiotracer was then eluted from the resin with acidified ethanol, which was filtered and diluted into an isotonic bicarbonate and saline solution. This efficiently buffered the pH of the final injectable solution and provided $[^{18}\text{F}]7$ as a concentrated, injectable solution for animal PET studies.

Dynamic microPET/CT imaging (with or without a saturating dose of TAK-875) was conducted in rats to evaluate tracer kinetics and the potential of [^{18}F]7 as an FFA-1-targeting agent. The images displayed high uptake of the tracer in abdominal organs. While tracer uptake could be detected in the pancreas ROI, there was no reduction in tracer retention in the TAK-875 pre-treatment group. This suggests that the signal from the pancreas is confounded by non-specific binding in the pancreatic tissue. To further understand the *in vivo* value of this tracer and confirm these results, the focus of investigation was shifted to the analysis of tissue samples *ex vivo*.

Ex vivo biodistribution studies have the added benefit of eliminating error introduced when drawing the microPET/CT pancreatic ROI, which is indistinguishable from surrounding organs and tissues in rodents by CT and could only be estimated based on known anatomy (Yin et al. 2015). These studies indicated very little uptake of the radiotracer in the fat, bone, and muscle tissues. [^{18}F]7 was detected in the pancreas (0.54 ± 0.04 tissue-to-blood ratio). However, saturating FFA-1 by pre-treatment with TAK-875 did not lead to a decrease in tracer accumulation in the pancreas, which corroborated the microPET results. This led to an examination of the formation and presence of potential radiolabeled metabolites to characterize the radioactive signal that accumulated in the pancreas. Interestingly, HPLC radio-metabolite analysis exhibited only the presence of unchanged [^{18}F]7 in the pancreas at 60-min post-injection. The formation of one minor metabolite was also detected in the plasma. Together with the absence of radioactivity accumulation in the bone in the biodistribution studies, this result confirmed the relatively high metabolic stability of [^{18}F]7 in rats.

During the course of this work, a study found that [^3H]TAK-875 exhibits a high level of off-target binding, likely related to the high degree of lipophilicity of the molecule ($\text{cLogP} = 4.2$) (Hellström-Lindhahl et al. 2017). Given the similarity of [^{18}F]7 with TAK-875 in terms of chemical structure and lipophilicity ($\text{cLogP} = 4.58$), and with the results described here, it can be concluded that non-specific binding of [^{18}F]7 in the pancreatic tissue invalidates this tracer as an *in vivo* or *ex vivo* quantitative FFA-1 imaging agent. Future development of TAK-875-derived FFA-1 targeting radiotracers should be approached with a focus on decreasing off-target labeling in the pancreas and surrounding tissue by increasing the hydrophilicity.

Conclusions

A one-pot, two-step fully automated process for the preparation of [^{18}F]7 was developed. The use of a pentafluorophenyl-functionalized HPLC column in this process allowed for the removal of the potential FFA-1 competitive impurity **8** and improved the purity and apparent molar activity of the final product. A strong anion-exchange resin was used to conduct rapid and efficient reformulation of the radiotracer in high concentration, enabling *in vivo* evaluation of [^{18}F]7 as a quantitative PET agent. MicroPET/CT imaging and biodistribution results exhibited activity accumulation in the pancreas although no specific binding could be detected following saturation studies of FFA-1 receptor. Radio-metabolite analysis indicated that [^{18}F]7 is sufficiently stable, ruling out the possibility that degradation was a contributing factor to the high degree of non-specific binding observed. While these results allow for the conclusion that non-specific binding of [^{18}F]7 in the pancreas impedes the ability to measure specific binding, they are instructive and provide direction for the development of future PET tracers for FFA-1-based β -cell PET imaging.

Abbreviations

AM: Accurate mass; CT: Computed tomography; EM: Expectation maximization; EOS: End of synthesis; ESI: Electrospray ionization; FFA: Free-fatty acid receptor; HPLC: High performance liquid chromatography; HR: High resolution; ID: Injected dose; NMR: Nuclear magnetic resonance; OSEM: Ordered subset expectation maximization; PET: Positron emission tomography; RCY: Radiochemical yield; ROI: Region of interest; SD: Standard deviation; SPECT: Single photon emission computed tomography; SUV: Standardized uptake value; T2DM: Type II diabetes mellitus; THF: Tetrahydrofuran

Acknowledgements

The authors thank the staff from the Radiochemistry and Cyclotron platform at the CRCHUM and Fleur Gaudette of the CRCHUM Pharmacokinetics core facility for high-resolution and accurate mass measurements.

Funding

Not applicable.

Availability of data and materials

All data generated or analysed during this study are included in this published article [and its supplementary information files].

Authors' contributions

MHD, JG, BB, VP, JND designed the study; MHD, DP, JMS, and AA performed the experiments. MHD, DP, JMS, AA, GX, and JND analyzed the data; MHD and JND wrote the manuscript. All authors read and approved the final manuscript.

Ethics approval

This study was carried out in accordance with Canadian Council on Animal Care guidelines. The protocol (protocol number IM16029JDSr) was approved by the institutional Animal Care Committees of the Centre de Recherche du Centre Hospitalier de l'Université de Montreal and the McGill University Health Centre.

Consent for publication

Not applicable.

Competing interests

The authors declare that they have no competing interests.

Publisher's Note

Springer Nature remains neutral with regard to jurisdictional claims in published maps and institutional affiliations.

Author details

¹Centre de Recherche du Centre Hospitalier de l'Université de Montréal, 900 rue St. Denis, Montréal, Québec H2X 0A9, Canada. ²Département de radiologie, radio-oncologie et médecine nucléaire, Université de Montréal, 2900 boulevard Edouard-Montpetit, Montréal, Québec H3T 1A4, Canada. ³Centre for Translation Biology, Research Institute of the McGill University Health Centre, 1001 boulevard Décarie-Block E, Montréal, Québec H4A 3J1, Canada. ⁴Département de médecine, Université de Montréal, 2900 boulevard Edouard-Montpetit, Montréal, Québec H3T 1A4, Canada.

Received: 3 October 2018 Accepted: 22 November 2018

Published online: 20 December 2018

References

- Andralojc K, Srinivas M, Brom M, Joosten L, de Vries IJM, Eizirik DL, et al. Obstacles on the way to the clinical visualisation of beta cells: looking for the Aeneas of molecular imaging to navigate between Scylla and Charybdis. *Diabetologia*. 2012; 55(5):1247–57.
- Bertrand R, Hamp I, Brönstrup M, Weck R, Lukacevic M, Polyak A, et al. Synthesis of GPR40 targeting ³H- and ¹⁸F-probes towards selective beta cell imaging. *J Label Comp Radiopharm*. 2016b;59(14):604–10.
- Bertrand R, Wolf A, Ivashchenko Y, Lo M, Scha M. Synthesis and characterization of a promising novel FFAR1/GPR40 targeting fluorescent probe for β -cell imaging. *ACS Chem Biol*. 2016a;11(6):1745–54.
- Briscoe CP, Tadayyon M, Andrews JL, Benson WG, Chambers JK, Eilert MM, et al. The orphan G protein-coupled receptor GPR40 is activated by medium and long chain fatty acids. *J Biol Chem*. 2002;278(13):11303–11.
- Hellström-Lindahl E, Åberg O, Ericsson C, O'Mahony G, Johnström P, Skrtic S, et al. Toward molecular imaging of the free fatty acid receptor 1. *Acta Diabetol*. 2017;54(7):663–8.
- Ionescu-Tirgoviste C, Gagniac PA, Gubceac E, Mardare L, Popescu I, Dima S, et al. A 3D map of the islet routes throughout the healthy human pancreas. *Sci Rep*. 2015;5:14634.
- Itoh Y, Kawamata Y, Harada M, Kobayash M, Fuji R, Fukusumi S, et al. Free fatty acids regulate insulin secretion from pancreatic beta-cells through GPR40. *Nature*. 2003;422:173–6.
- Kahn SE. The relative contributions of insulin resistance and beta-cell dysfunction to the pathophysiology of type 2 diabetes. *Diabetologia*. 2003;46(1):3–19.
- Kenk M, Greene M, Lortie M, Robert A, Beanlands RS, Dasilva JN. Use of a column-switching high-performance liquid chromatography method to assess the presence of specific binding of (R)- and (S)-[¹¹C]rolipram and their labeled metabolites to the phosphodiesterase-4 enzyme in rat plasma and tissues. *Nucl Med Biol*. 2008;35(4):515–21.
- Mancini AD, Poitout V. GPR40 agonists for the treatment of type 2 diabetes: life after "TAKing" a hit. *Diabetes Obes Metab*. 2015;17(7):622–9.

- Negoro N, Sasaki S, Mikami S, Ito M, Suzuki M, Tsujihata Y, et al. Discovery of TAK-875: a potent, selective, and orally bioavailable GPR40 agonist. *ACS Med Chem Lett.* 2010;1(6):290–4.
- Negoro N, Sasaki S, Mikami S, Ito M, Tsujihata Y, Ito R, et al. Optimization of (2,3-Dihydro-1-benzofuran-3-yl)acetic acids: discovery of a non-free fatty acid-like, highly bioavailable G protein-coupled receptor 40/free fatty acid receptor 1 agonist as a glucose-dependent Insulinotropic agent. *J Med Chem.* 2012;55(8):3960–74.
- Otieno MA, Snoeys J, Lam W, Ghosh A, Player MR, Poci A, et al. Fasiglifam (TAK-875): mechanistic investigation and retrospective identification of hazards for drug induced liver injury. *Toxicol Sci.* 2017;163(2):1–11.
- Srivastava A, Yano J, Hirozane Y, Kefala G, Gruswitz F, Snell G, et al. High-resolution structure of the human GPR40 receptor bound to allosteric agonist TAK-875. *Nature.* 2014;513(7516):124–7.
- Wilke BI, Dornan MH, Yeung J, Boddy CN, Pinto A. Hexanes/acetonitrile : a binary solvent system for the efficient monosilylation of symmetric primary and secondary diols. *Tetrahedron Lett.* 2014;55(16):2600–2.
- Yin T, Coudyzer W, Peeters R, Liu Y, Cona MM, Feng Y, et al. Three-dimensional contrasted visualization of pancreas in rats using clinical MRI and CT scanners. *Contrast Media Mol Imaging.* 2015;10(5):379–87.

Submit your manuscript to a SpringerOpen[®] journal and benefit from:

- ▶ Convenient online submission
- ▶ Rigorous peer review
- ▶ Open access: articles freely available online
- ▶ High visibility within the field
- ▶ Retaining the copyright to your article

Submit your next manuscript at ▶ springeropen.com
